

## Uptake of heavy metal ions in layered double hydroxides and applications in cementitious materials

### Experimental evidence and first-principle study

Li, Bo; Zhang, Shizhe; Li, Qiu; Li, Neng; Yuan, Bo; Chen, Wei; Brouwers, H.J.H.; Yu, Qingliang

**DOI**

[10.1016/j.conbuildmat.2019.06.135](https://doi.org/10.1016/j.conbuildmat.2019.06.135)

**Publication date**

2019

**Document Version**

Final published version

**Published in**

Construction and Building Materials

**Citation (APA)**

Li, B., Zhang, S., Li, Q., Li, N., Yuan, B., Chen, W., Brouwers, H. J. H., & Yu, Q. (2019). Uptake of heavy metal ions in layered double hydroxides and applications in cementitious materials: Experimental evidence and first-principle study. *Construction and Building Materials*, 222, 96-107. <https://doi.org/10.1016/j.conbuildmat.2019.06.135>

**Important note**

To cite this publication, please use the final published version (if applicable). Please check the document version above.

**Copyright**

Other than for strictly personal use, it is not permitted to download, forward or distribute the text or part of it, without the consent of the author(s) and/or copyright holder(s), unless the work is under an open content license such as Creative Commons.

**Takedown policy**

Please contact us and provide details if you believe this document breaches copyrights. We will remove access to the work immediately and investigate your claim.

**Green Open Access added to [TU Delft Institutional Repository](#)  
as part of the Taverne amendment.**

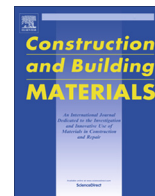
More information about this copyright law amendment  
can be found at <https://www.openaccess.nl>.

Otherwise as indicated in the copyright section:  
the publisher is the copyright holder of this work and the  
author uses the Dutch legislation to make this work public.



Contents lists available at ScienceDirect

# Construction and Building Materials

journal homepage: [www.elsevier.com/locate/conbuildmat](http://www.elsevier.com/locate/conbuildmat)

## Uptake of heavy metal ions in layered double hydroxides and applications in cementitious materials: Experimental evidence and first-principle study

Bo Li <sup>a,b,1</sup>, Shizhe Zhang <sup>c,1</sup>, Qiu Li <sup>a,b</sup>, Neng Li <sup>a,b,d</sup>, Bo Yuan <sup>b</sup>, Wei Chen <sup>a,\*</sup>, H.J.H. Brouwers <sup>a,b,e,\*</sup>, Qingliang Yu <sup>e</sup>

<sup>a</sup>State Key Laboratory of Silicate Materials for Architectures, Wuhan University of Technology, Wuhan, PR China

<sup>b</sup>School of Material Science and Engineering, Wuhan University of Technology, Wuhan, PR China

<sup>c</sup>Microlab, Faculty of Civil Engineering and Geosciences, Delft University of Technology, Delft, The Netherlands

<sup>d</sup>Research Center for Materials Genome Engineering, Wuhan University of Technology, Wuhan, PR China

<sup>e</sup>Department of the Built Environment, Eindhoven University of Technology, Eindhoven, The Netherlands

### H I G H L I G H T S

- Cu<sup>2+</sup> or Cr<sup>3+</sup> ions are immobilized with calcined Mg-Al LDHs.
- Cu<sup>2+</sup> or Cr<sup>3+</sup> enters the plate of LDHs forming a non-stoichiometric structure.
- Using slag can potentially mitigate the risk of heavy metal leaching by forming LDHs.

### A R T I C L E I N F O

#### Article history:

Received 8 March 2019

Received in revised form 3 June 2019

Accepted 17 June 2019

Available online 21 June 2019

#### Keywords:

Layered double hydroxides

Heavy metal ions

Solid state NMR

First principle calculation

### A B S T R A C T

The uptake mechanism of heavy metal ions in layered double hydroxides (LDHs) is investigated in this paper via solid-solution exchange experiments and first principle study. The uptake capacities of C-LDHs for heavy metal ions from solutions are experimentally investigated and the structures of LDHs doped with various heavy metal ions are revealed. The doped structures of LDHs are further re-established with first principle calculations. The results show that Cu<sup>2+</sup> or Cr<sup>3+</sup> ions are immobilized in the form of isomorphic substitution for Mg<sup>2+</sup> and Al<sup>3+</sup> in the plate of the layered structure, respectively, during reconstruction of calcined LDHs, forming a non-stoichiometric structure. The structure of the Cu<sup>2+</sup> doped LDHs is identified as  $[\text{Mg}_{(1-x)(1-z)}\text{Cu}_{(1-x)z}\text{Al}_x^{3+}(\text{OH})_2] \text{A}_{x/n}^{n-} \cdot y\text{H}_2\text{O}$ , where  $z$  is the molar ratio of Cu<sup>2+</sup> to Mg<sup>2+</sup>. The structure of Cr<sup>3+</sup> doped LDHs is identified as  $[\text{Mg}_{1-x}\text{Cr}_{xz}\text{Al}_{x(1-z)}^{3+}(\text{OH})_2] \text{A}_{(x+z)/n}^{n-} \cdot y\text{H}_2\text{O}$ , where  $z$  is the molar ratio of Cr<sup>3+</sup> to Al<sup>3+</sup>. The Cu<sup>2+</sup> or Cr<sup>3+</sup> ions in the hardened cement paste modified with calcined Mg-Al LDHs as immobilizing admixture can be efficiently removed from the pore solution and chemically stabilized in the structure of LDHs.

© 2019 Elsevier Ltd. All rights reserved.

### 1. Introduction

Heavy metal ion contamination of surrounding soil or groundwater from industrial and municipal solid wastes has been a major concern in the treatment of solid wastes globally [1–3]. Heavy metal ions are persistent environmental contaminants since they cannot be degraded or destroyed by biological metabolism [4].

\* Corresponding authors at: State Key Laboratory of Silicate Materials for Architectures, Wuhan University of Technology, Wuhan, PR China (W. Chen).

E-mail addresses: [chen.wei@whut.edu.cn](mailto:chen.wei@whut.edu.cn) (W. Chen), [jos.brouwers@tue.nl](mailto:jos.brouwers@tue.nl) (H.J.H. Brouwers).

<sup>1</sup> These authors contribute equally to this study.

Therefore, heavy metal ions are reported as prior threats to human health and ecosystem due to their biological toxicity and metabolic stability [5].

Immobilization and stabilization of heavy metal contaminated wastes with cement has been well established as an efficient technique for minimizing their environmental impacts with the advantages of high strength, low permeability and high durability [6–8]. Meanwhile, whether the heavy metal ions in the wastes can be reliably immobilized to the greatest degree in the process of cement hydration remains as one of the major uncertainties [9–11].

Stabilization and solidification of heavy metal ions with Portland cement was first proposed for the solidification of nuclear wastes in the 1950s [9]. Heavy metal ions accelerates the

dissolution of Portland cement clinker, but retards the precipitation of portlandite and calcium silicate hydrate (C-S-H), resulting in prolonged setting time, low strength and high porosity [5]. Mineral additives such as fly ash (FA), ground granulated blast furnace slag (GGBFS) and metakaolin (MK) are added into cement that increases the strength and lowers the permeability of the matrix, which promotes the immobilization degree of heavy metal ions [11,12]. Alkali-activated slag binders are more advantageous for immobilizing heavy metal ions owing to the higher amount of gel pores and less capillary pores than ordinary Portland cement pastes. Some extra negative charges are introduced into C-A-S-H gels due to the substitution of  $\text{Si}^{4+}$  by  $\text{Al}^{3+}$  to form  $\text{Q}^n(\text{Al})$  sites. Heavy metal ions are absorbed and immobilized into the cementitious matrix by electrostatic attraction, since these heavy metal ions show strong adsorption abilities in  $\text{Q}^n(\text{Al})$  sites [13,14].

Layered double hydroxides (LDH), also known as hydrotalcite-like materials are a family of materials characterized by a layered structure with the generic layer sequence  $[\text{AcBZAcB}]_n$ , where c represents layers of metal cations, A and B are layers of hydroxide ( $\text{OH}^-$ ) anions, and Z are layers of other anions and neutral molecules (such as water). The chemical formula of LDHs can be represented with a general formula  $[\text{M}_1^{2+}_x\text{M}_2^{3+}_y(\text{OH})_z]_n \text{A}^{n-}_x \cdot y\text{H}_2\text{O}$ , where  $\text{M}^{2+}$  and  $\text{M}^{3+}$  are divalent and trivalent metal cations,  $\text{A}^{n-}$  is the interlayer anions and x is the  $\text{M}^{3+}/(\text{M}^{2+} + \text{M}^{3+})$  molar ratio [15]. The layered structure of LDHs is built by periodical stacking of positively charged  $(\text{M}^{2+}, \text{M}^{3+})(\text{OH})_6$  octahedral plates similar to brucite and is negatively charged by interlayer groups consisting of anions. LDHs have attracted considerable attention for removal of environmental contaminants from surrounding solution owing to their ion-exchange capacities and structure reconstruction abilities [16,17].

One-half of magnesium in the plate of LDHs lattice can be replaced with other cations in the process of structural reconstruction [18]. LDHs can remove  $\text{Cu}^{2+}$  and  $\text{Pb}^{2+}$  from aqueous solution and the main mechanisms are found to be surface adsorption and precipitation [19]. LDHs modified with organic acid anions such as citrate<sup>3-</sup>, malate<sup>2-</sup>, and tartrate<sup>2-</sup> can immobilize heavy

metal ions through chelation reactions [20]. The  $\text{M}^{2+}$  metal cations in the plate of Mg-Al LDHs exchanges with the transition metal ions such as  $\text{Co}^{2+}$ ,  $\text{Ni}^{2+}$  or  $\text{Zn}^{2+}$  forming  $[\text{M}^{2+}, \text{Mg}]_2\text{Al}(\text{OH})_6\text{Cl}$  [21,22].

Five main processes including physical inclusion, precipitation, surface adsorption, isomorphous substitution and chelation reaction are concluded in existing literature as the uptake mechanisms of heavy metal ions in LDHs (Fig. 1) [8,22,23]. In the isomorphous substitution and chelation reaction processes, the heavy metal ions are immobilized into the main plate and interlayer space of LDHs, respectively. Carbonation reaction of chelated LDHs releases the interlayer heavy metal ions because the carbonate anion has strongest affinity in the interlayer space of LDHs [24]. Isomorphous substitution of heavy metal ions in the plate of LDHs is thus expected to be the most stable and reliable process for immobilization.

Identifying the location of heavy metal ions in the structure of LDHs after exchanges is important for understanding the uptake mechanism and maximizing the immobilization capacities of LDHs. Identifying the location of these ions in LDHs and consequently the molecular structure of the modified LDHs requires a comprehensive investigation on the interaction of atoms in the plate structures. Nuclear magnetic resonance (NMR) analysis is an important technique for revealing the chemical environments surrounding specific atomic nucleus and the short-range order in the material. NMR studies of LDHs are particularly attractive due to the abundance of spin-active nuclei from which site-specific structural information can be potentially extracted [25].

First principle calculations based on the Density Functional Theory (DFT) employing the Gauge Including Projector Augmented Wave (GIPAW) algorithm enable the calculation of chemical shielding, which establishes a clear link between the observed spectra and underlying molecular structure [26–28]. Combined with NMR tests and first principle calculation for NMR results, the exact chemical environment of heavy metals and atomic structures of LDHs after immobilization can be identified. First principle calculations have been proven to be a useful tool for promoting the understanding on the absorption mechanism and adsorption capacity of many absorption process [29,30] when the exact chemical environment of atoms in the structure can be identified.

One of the unique properties of LDHs is that after being calcinated and re-mixed with water, they can restore the layered structure. LDHs lose the surface and interstitial water if heated below 250 °C, followed by decomposition of the interlayer anion groups and dehydroxylation of the plates if further heated to 450 °C [22]. The partially or fully dehydrated C-LDHs will rehydrate with water and anions to reform the layered structure with great fidelity, which are illustrated by Fig. 2 [31].

Calcined LDHs are a kind of positive charge material on surface with higher isoelectric points [32]. Very little work has been done on the uptake mechanism of calcined LDHs for heavy metal ions in the reconstruction process, though it has been found that the calcined LDHs are much more efficient than the virgin ones [22,32]. There is a potential inference that the distorted plates in LDHs after

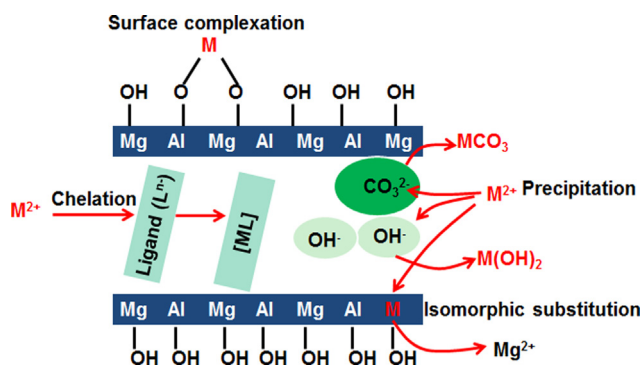


Fig. 1. Schematic representation of the uptake mechanisms, reproduced from ref. [23].

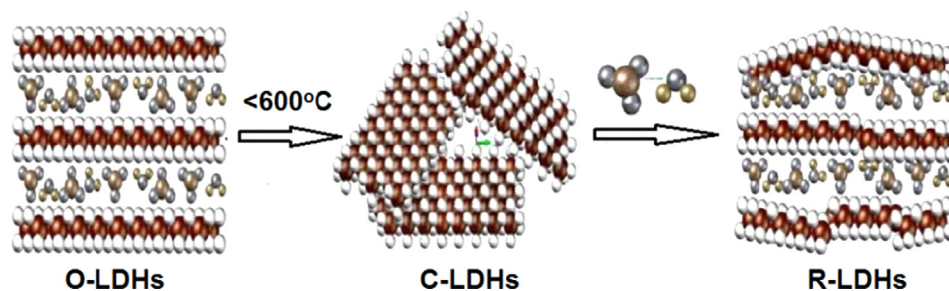


Fig. 2. Illustration for the rehydration process of C-LDHs to form R-LDHs, reproduced from ref. [32].

calcination can uptake heavy metal ions through isomorphous substitution process during its rehydration [32,33], which still lacks some evidences.

LDHs is a common hydration product of cement containing vitreous slags rich in magnesium, e.g. ground granulated blast furnace slag, nickel slag, manganese slag or others [34,35]. Some of these vitreous slags may contain high amounts of heavy metals as well, shielding great potential risk for their use in cement production [36–38]. The LDHs form simultaneously in the hydration process of cement containing Mg rich slag, making it potentially a promising candidate for immobilizing heavy metal ions parallel to the hardened process of concrete. The efficiency of LDHs for immobilizing heavy metal ions in cement-based materials is thus greatly interesting for evaluating the risks of using heavy metal containing Mg-rich slags in cement.

The uptake mechanism of heavy metal ions in calcined LDHs during the rehydration process are studied in this paper. The inter-atomic interactions and the consequent atomic rearrangements in the plate of LDHs after the rehydration process are revealed experimentally with NMR analysis based on outputs of first-principle calculations. The uptake mechanism of heavy metal ions in LDHs is thus established and molecular structural model of the modified LDHs is proposed. The feasibility of using LDHs as an immobilization agent for heavy metal ions in cement-based materials is explored.

## 2. Materials and experiments

### 2.1. Materials

Mg-Al- $\text{CO}_3$  LDHs is prepared with a co-precipitation method using  $\text{Mg}(\text{NO}_3)_2 \cdot 6\text{H}_2\text{O}$ ,  $\text{Al}(\text{NO}_3)_3 \cdot 9\text{H}_2\text{O}$ , NaOH and  $\text{Na}_2\text{CO}_3$  [2,24,39]. An aqueous solution containing 2 M  $\text{Mg}(\text{NO}_3)_2 \cdot 6\text{H}_2\text{O}$  and 1 M  $\text{Al}(\text{NO}_3)_3 \cdot 9\text{H}_2\text{O}$  is added dropwise into a solution containing 3.4 M NaOH and 1 M  $\text{Na}_2\text{CO}_3$ . The volumetric ratio of the solution containing  $\text{Mg}(\text{NO}_3)_2 \cdot 6\text{H}_2\text{O}$  and  $\text{Al}(\text{NO}_3)_3 \cdot 9\text{H}_2\text{O}$  to the solution containing NaOH and  $\text{Na}_2\text{CO}_3$  is 0.50. The resulting slurry is matured at 70 °C for 24 h followed by filtration and washing with deionized water. The filtrate is dried at 120 °C [24] and ground in a cradle into fine powder with particle sizes smaller than 80  $\mu\text{m}$ . The synthetic Mg-Al- $\text{CO}_3$  LDHs is hereafter referred to as O-LDHs.

The O-LDHs is calcined in a muffle furnace with a heating rate of 3 °C/min up to 550 °C and continuously calcined for 5 h. The calcined powder is cooled in the furnace to the ambient temperature and is then also ground in a cradle into fine powder with particle sizes smaller than 80  $\mu\text{m}$ , hereafter referred to as C-LDHs.

C-LDHs is mixed with saturated calcium hydroxide solution in the air, and stirred continuously for 24 h. The solid precipitate is collected by filtration and dried at 105 °C for 24 h in vacuum and ground into powder, hereafter referred to as R-LDHs.

The chemical compositions of the three types of LDHs (namely O-LDHs, C-LDHs, R-LDHs) analyzed with X-ray fluorescence (XRF, Model Axios Advanced) technique are listed in Table 1. The main difference among the compositions of the three types LDHs is the loss on ignition (LOI), which corresponds to the volatile contents

containing  $\text{CO}_3^{2-}$  and  $\text{OH}^-$  in O-LDHs and R-LDHs. The molar ratio or Mg to Al in three types of LDHs varies in a small range close to 2.0, probably due to technical limits of the XRF technique.

The three types of LDHs are analyzed with X-ray diffraction technique (XRD, Model Rigaku MiniFlex600, Cu  $K\alpha$ , incident radiation, 0.2°/min) and the results are shown in Fig. 3. The structure of O-LDHs is identified as hydrotalcite with good crystalline state. The layered structure of O-LDHs is degraded after being calcined at 550 °C and no crystalline phases are identified in the XRD pattern. After rehydration of C-LDHs, the layered structure reforms and the characteristic peaks of hydrotalcite appear but with a lower intensity, indicating a poor crystallinity. This structure reconstruction ability has been extensively used to absorb  $\text{CO}_3^{2-}$ ,  $\text{SO}_4^{2-}$  and  $\text{Cl}^-$  by Mg-Al LDHs or Ca-Al LDHs to improve the durability of cementitious materials [24,34,40,41].

The particle size distributions of O-LDHs, C-LDHs and R-LDHs analyzed with a laser particle size analyzer (Model Malvern Mastersizer 2000) are shown in Fig. 4. The average particle size of O-LDHs, C-LDHs and R-LDHs are 13.43  $\mu\text{m}$ , 14.89  $\mu\text{m}$  and 12.56  $\mu\text{m}$ , respectively. C-LDHs have relatively larger particle sizes than the other two types of LDHs, suggesting the C-LDHs particles are agglomerated and are more difficult to disperse than the other two types of LDHs.

### 2.2. Experiments

C-LDHs are used in the immobilization experiment of heavy metal ions in aqueous solution to explore the possibilities of uptake heavy metal ions through isomorphous substitution in the rehydration process. A sodium chloride solution with concentration of 0.5 mol/L is prepared. Heavy metal solutions with 5 mM

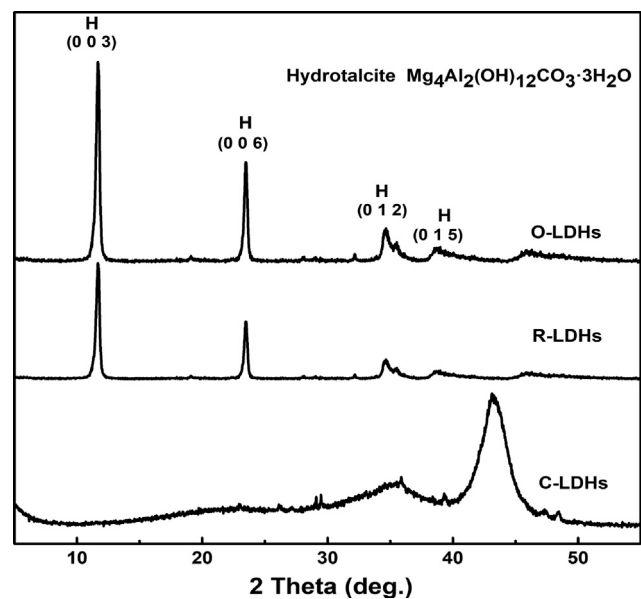


Fig. 3. XRD patterns of O-LDHs, C-LDHs and R-LDHs.

Table 1  
Oxides composition of LDHs and Portland cement (mass %).

Oxide	$\text{SiO}_2$	$\text{Al}_2\text{O}_3$	$\text{Fe}_2\text{O}_3$	CaO	MgO	$\text{Na}_2\text{O}$	$\text{SO}_3$	$\text{K}_2\text{O}$	L.O.I.	Mg/Al molar ratio
O-LDH	–	20.75	–	–	34.27	1.80	–	–	41.02	2.11
C-LDH	–	34.72	–	–	55.07	2.64	–	–	4.17	2.02
R-LDH	–	22.46	–	–	35.18	0.45	–	–	38.57	2.00
Portland Cement	21.5	5.86	2.85	59.81	2.23	0.20	2.06	0.67	3.70	–

Note: “–”, not detected.

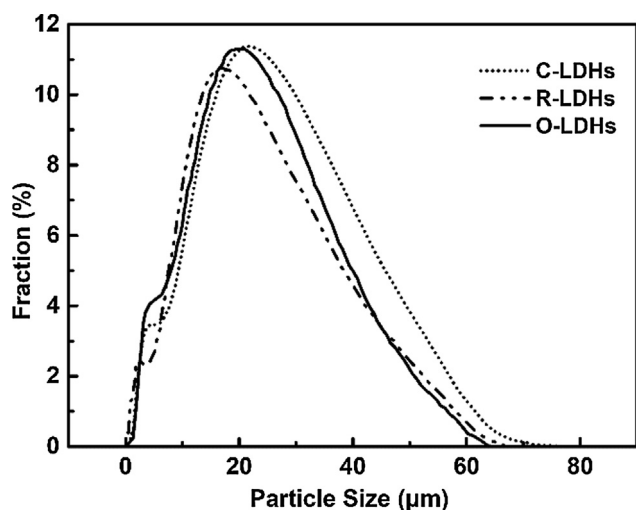


Fig. 4. Particle size distribution of LDHs powder before and after treatment.

and 10 mM concentrations are prepared by dissolving  $\text{CuCl}_2 \cdot 2\text{H}_2\text{O}$  or  $\text{CrCl}_3 \cdot 6\text{H}_2\text{O}$  in the sodium chloride solution. The initial concentration of heavy metal ions have large effect on the uptake efficiency. The concentration of heavy metal ions in real environmental pollutants is much lower than that in the experiments, leading to reduced uptake efficiency by LDHs [22,42]. A combined system with C-LDHs and electrokinetic methods has been applied for Cr(VI)-contaminated soil remediation [43] to increase the uptake efficiency in the practical application. Thus, some combined methods is promising in the in the practical application.

The  $\text{Cu}^{2+}$  ions will precipitate and form  $\text{Cu}(\text{OH})_2$  in solutions if the pH value is higher than 6.5 [44]. Similarly,  $\text{Cr}^{3+}$  ions will precipitate and form  $\text{Cr}(\text{OH})_3$  in solutions if the pH value is higher than 6.8 [45]. The pH value of the solutions containing heavy metal ions is thus adjusted to 4.0 to assure that the heavy metal ions will not precipitate out of the solution after equilibrium with C-LDHs. The pH value is adjusted by adding 0.1 M NaOH solution or 0.1 M hydrochloric acid into the solution till the pre-determined value.

Experiments on uptake capacities of C-LDHs to  $\text{Cu}^{2+}$  or  $\text{Cr}^{3+}$  ions are performed with solid-solution exchange tests. 2 g of C-LDHs and 500 mL solution containing heavy metal ions are mixed together in a polythene bottle and are placed into a horizontal agitator for 24 h. The aqueous phase is separated by centrifugation after 12 h and the final concentration of metal ions in the solution is determined with Inductively Coupled Plasma (ICP, Model Optima 4300DV). The amount of immobilized metal ions is calculated from the difference between the initial and final concentrations and the volume of the solution. The filtrate is dried at 60 °C for 24 h and tested with XRD, X-ray photoelectron spectroscopy and Nuclear magnetic resonance (NMR). Transmission electron microscopy (TEM Mode JEM-1400Plus, 120 kV) is used for structural analysis of rehydrated C-LDHs in  $\text{Cr}^{3+}$  solution.

Kinetic experiment on uptake of  $\text{Cu}^{2+}$  by reconstruction of C-LDHs in a solution is performed at 25 °C. 50 mL aqueous solution containing  $\text{Cu}^{2+}$  ions (concentration 0.4 mM) is prepared by dissolving  $\text{CuCl}_2 \cdot 2\text{H}_2\text{O}$  into deionized water. The pH value is adjusted to 4 using 0.1 M HCl solution. 100 mg C-LDHs is added into 50 mL aqueous solution. At given time intervals, the solutions are centrifuged and the supernatants are analyzed for metal ions concentration with ICP.

The uptake capacities of C-LDHs modified cement mortar are investigated. Portland cement mortar specimens with a water/cement ratio of 0.50 and cement/sand ratio of 1/3 are prepared

for the immobilization experiment of heavy metal ions. The oxide composition of a Portland cement complying with the Chinese Standard GB/T 175-2007 is listed in Table 1. C-LDHs are added to cement with a dosage of 5% to the cement by mass. Solutions with a concentration of 5 mM are prepared by dissolving  $\text{CuCl}_2 \cdot 2\text{H}_2\text{O}$  or  $\text{CrCl}_3 \cdot 6\text{H}_2\text{O}$  into deionized water. The solution is used as mixed water when preparing the cement mortar. The mortar without C-LDHs addition is used as reference sample. The fresh mortar is casted into  $40 \times 40 \times 160 \text{ mm}^3$  steel moulds and cured for 24 h followed by de-moulding. The specimens are cured for 14 days at  $20 \pm 3 \text{ }^\circ\text{C}$  and relative humidity above 95% RH. Compressive strength of plain mortar and LDHs modified mortar are tested according to the Chinese standard GB/T 17671-1999 with a fixed loading rate at 2.4 kN/s.

The leaching rate of heavy metal ions out of the hardened mortar is determined following the procedure given in the standard GB5086.2-1997. The hardened mortar specimens are crushed and about 20 g particles with sizes between 5 and 6 mm are collected. The mortar particles are mixed with de-ionized water with a water to solid mass ratio of 20, and placed into sealed glass bottles. The bottles containing mortar and solution are fixed onto a horizontal agitator and shaken with a frequency of  $110 \pm 10$  times/min for 8 h to extract ions from the hardened mortar. The mixture is then filtered and the filtrates are collected. The pH of the filtrates is adjusted to 2 with HCl solution before measuring the concentration of leached heavy metal ions with ICP for preventing precipitation out of solution.

Portland cement pastes are prepared for investigating the mechanism of effective immobilization of heavy metal ions by C-LDHs in cement materials. Paste samples are prepared with a water/cement ratio of 0.40. Heavy metal ions solutions containing 5 mM  $\text{CuCl}_2 \cdot 2\text{H}_2\text{O}$  or  $\text{CrCl}_3 \cdot 6\text{H}_2\text{O}$  are used as mix water when preparing the cement paste. C-LDHs are added to cement with a dosage of 5% by mass to the cement. The fresh paste is casted into moulds sizing  $20 \times 20 \times 20 \text{ mm}^3$ . The paste is cured for 14 days and is then ground to fine powders with particle sizes smaller than 80  $\mu\text{m}$ . The paste powder is analyzed with XRD and NMR.

### 2.3. Analysis techniques

XPS spectra are recorded on an ESCALAB 250Xi instrument.  $\text{Al}_{K\alpha}$  X-ray beam (1486.6 eV) is generated from an aluminum rotating anode. C 1 s peak of the surface adventitious carbon at 284.6 eV is used as reference for the binding energies of  $\text{Cr}^{3+}$  2p and  $\text{Cu}^{2+}$  2p.

$^{27}\text{Al}$  and  $^1\text{H}$  magic angle spinning (MAS) NMR spectra are recorded on an Agilent 600 DD2 spectrometer, equipped with a 14.1 T magnet, operating at a Larmor frequency of 600 MHz. The experiments use a 4.0 mm double resonance 1H-X MAS probe and a spinning frequency of 12.0 kHz for  $^{27}\text{Al}$  and 15.0 kHz for  $^1\text{H}$ .  $\text{AlCl}_3$  salt and tetramethylsilane are used as reference for  $^{27}\text{Al}$  and  $^1\text{H}$ , respectively.

### 2.4. First principle calculations

The first principle calculations are performed with CASTEP (Accelrys, Material Studio17.2) using DFT in the generalized gradient approximation GGA PBE function with plane wave basis [46]. The calculation is executed in three steps: geometry optimization, energy calculation and chemical shielding calculation [47]. Geometry optimization and energy calculation are carried out within CASTEP using a k point grip of  $3 \times 3 \times 1$  and cut off energy of 500 eV. The core-valence interactions are described by ultrasoft pseudopotentials. Little changes of unit cell and atomic positions are allowed during geometry optimization.  $^1\text{H}$  chemical shielding calculation is performed in the crystal frame. All-electron wave function in the presence of a magnetic field is reconstructed with

the gauge including projector augmented wave (GIPAW) algorithm [26]. A  $k$  point grid of  $3 \times 3 \times 1$  and cut off energy of 400 eV are used. The chemical shifts  $\delta_{cal}$  are obtained from chemical shielding  $\sigma_{cal}$  with the relation:

$$\delta_{cal} = \sigma_{ref} - \sigma_{cal} \quad (1)$$

where the value of  $\sigma_{ref}$  for  $^1\text{H}$  is 30.09 ppm.

### 3. Results and discussion

#### 3.1. Uptake of heavy metal ions in aqueous solutions

Ion concentrations of the solutions with an initial heavy metal ions concentration of 5 mM and 10 mM after reacting with C-LDHs are listed in Table 2. The uptake capacity of C-LDHs for different ions is evaluated with a parameter named uptake efficiency ( $U_e$ ) that is calculated from the initial and final concentrations after solution-solid interactions with the Eq. (2) as:

$$U_e = \frac{(C_{initial} - C_{final})}{C_{initial}} \times 100\% \quad (2)$$

in which  $U_e$  is the uptake efficiency (%),  $C_{initial}$  (mM) is the initial concentration of ion in the solution and  $C_{final}$  (mM) is the concentration after interaction.

It can be concluded from Table 2 that the heavy metal ions  $\text{Cu}^{2+}$  or  $\text{Cr}^{3+}$  are immobilized during rehydration of C-LDHs. The uptake efficiencies are affected by the initial concentration and nature of the ion. C-LDHs exhibits the best immobilization capacity with  $\text{Cu}^{2+}$  ion of which the uptake efficiencies reach 90.66% and 60.44% for the initial concentration of 5 mM and 10 mM, respectively. The uptake efficiency of  $\text{Cr}^{3+}$  ion up to 30% is observed in the experiments.

The uptake efficiency of  $\text{Cu}^{2+}$  ion in hydrating C-LDHs after different hydration time is shown in Fig. 5. The uptake efficiency increases rapidly during the first two hours, reaching 90.16%. The uptake efficiency reaches 90.6% after about 5 h, indicating an uptake capacity at equilibrium ( $q_e$ ) of 11.3 mg/g which is calculated from Eq. (3).

$$q_e = \frac{U_e \times C_{initial} \times V}{m} \quad (3)$$

where  $q_e$  is the uptake capacity at equilibrium (mg/g);  $V$  is the volume (L);  $m$  is the mass of C-LDHs (g).

The pseudo-first order and pseudo-second order model are used to investigate the kinetic characteristics of the  $\text{Cu}^{2+}$  uptake in C-LDHs [42]. The pseudo-first order kinetic and pseudo-second order kinetic model are shown as Eqs. (4) and (5), respectively.

$$\ln(q_e - q_t) = \ln q_e - K_1 t \quad (4)$$

$$\frac{t}{q_t} = \frac{1}{K_2} + \frac{1}{q_e} t \quad (5)$$

where  $t$  is the reaction time (min);  $q_t$  is the amount of  $\text{Cu}^{2+}$  ions removed at time  $t$  (mg/g);  $q_e$  is the uptake capacity at equilibrium (mg/g);  $K_1$  and  $K_2$  are the rate constants of pseudo-first order kinetic model and pseudo-second kinetic model (1/min), respectively.

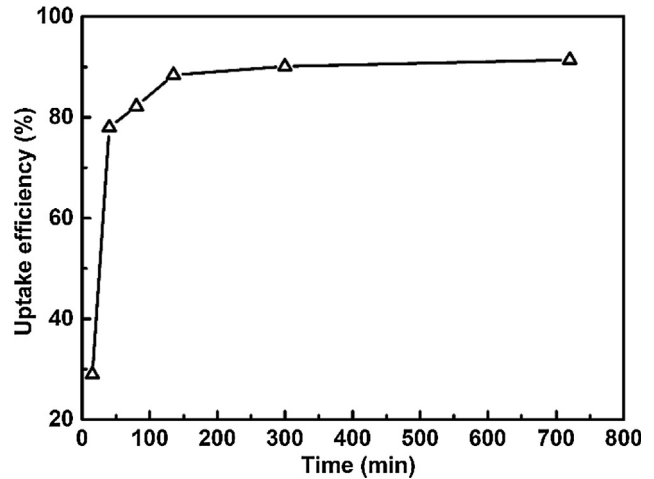


Fig. 5. Uptake efficiency of  $\text{Cu}^{2+}$  ion in hydrating C-LDHs (Initial concentration of 0.4 mM).

These two kinetic models are applied and fitted with experiment data, which are shown in Fig. 6a and b. The theoretical  $q_e$  value calculated from the pseudo-second order kinetic model is 11.63 mg/g, which matches well with the experimental values. These results show that the reaction of C-LDHs with  $\text{Cu}^{2+}$  ions follows the pseudo second-order type kinetic reaction based on the assumption that the rate-limiting step is chemical sorption involving valency forces through sharing or exchange of electrons between sorbent and sorbate [48].

Uptake efficiency of around 70% in O-LDHs for  $\text{Cu}^{2+}$  was reported and around 100% in humate-modified LDHs through chelation reaction [19,48]. By using C-LDHs, the uptake efficiency of  $\text{Cu}^{2+}$  is obviously promoted compared to the virgin LDHs (O-LDHs). As discussed previously, the immobilization process of heavy metal ions through the chelation reaction is reversible if the LDHs are carbonated. It is therefore more reliable to use the O-LDHs or the C-LDHs to immobilize the ions through isomorphic substitution, which is clarified further in this study.

#### 3.2. Mechanism of heavy metal ion uptake in C-LDHs

When the heavy metal ions contact with C-LDHs, these metal ions firstly generated hydroxide precipitation onto the surface. There is a potential inference that some metal ions can transfer into the structure when the C-LDHs reconstruct the layered structure followed by surface absorption [32,33]. The mechanism of immobilization of heavy metal ions with C-LDHs is investigated through XRD, TEM, NMR and first principle calculations in this paper.

XRD patterns of rehydrated C-LDHs after reaction with  $\text{Cu}^{2+}$  or  $\text{Cr}^{3+}$  solutions are shown in Fig. 7. The broadening of characteristic peaks of LDHs with heavy metal immobilization compared with O-LDHs can be observed in XRD pattern, which is possibly due to decreased crystallinity during the rehydration process of C-LDHs.

Table 2  
Ion concentrations of solutions after reaction with LDHs.

Ions	Initial concentration (mM)	Final concentration (mM)	Change of concentration (mM)	Uptake efficiency (%)
$\text{Cu}^{2+}$	5.0	0.467	4.533	90.66
$\text{Cr}^{3+}$		2.646	2.354	47.07
$\text{Cu}^{2+}$	10	3.956	6.044	60.44
$\text{Cr}^{3+}$		6.970	3.030	30.30

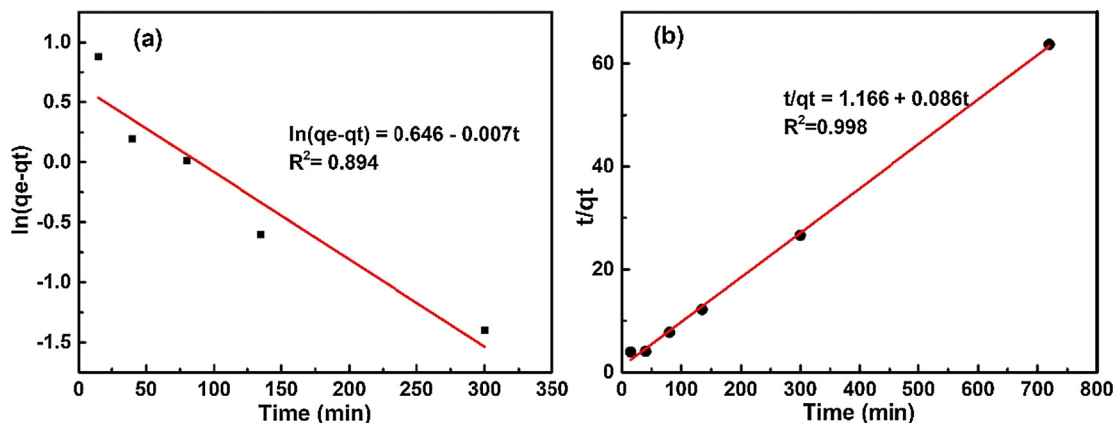


Fig. 6. Fitness of the kinetic curve of LDH reacting with Cu<sup>2+</sup> ion (Initial concentration of 0.4 mM). (a) pseudo first-order model, (b) pseudo second-order model.

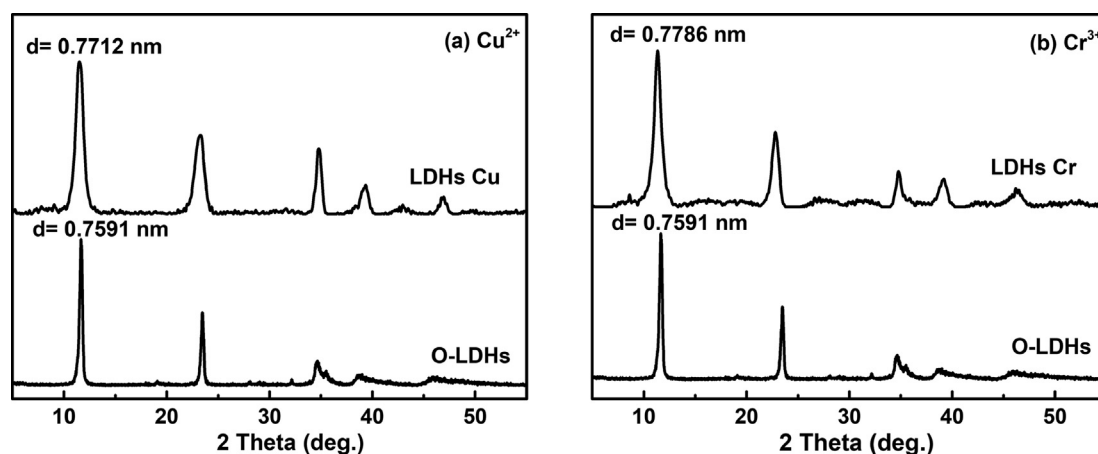


Fig. 7. XRD patterns of rehydrated C-LDHs after reaction with Cu<sup>2+</sup> or Cr<sup>3+</sup> solution (Initial concentration of 5 mM). (a) Cu<sup>2+</sup> solution, (b) Cr<sup>3+</sup> solution.

The diffraction peaks of C-LDHs reacting with Cu<sup>2+</sup> or Cr<sup>3+</sup> ions are similar to that of O-LDHs, indicating the structure of rehydrated C-LDHs with presence of Cu<sup>2+</sup> or Cr<sup>3+</sup> solution is identical to the original LDHs before calcination. No metal hydroxides and metal carbonates are detected which agrees with literature [19,48]. No new phases containing heavy metal ions are detected in XRD patterns in Fig. 7a and b. Cu<sup>2+</sup> or Cr<sup>3+</sup> ions are supposed to be incorporated in the layered structure of LDHs. It can be observed from Fig. 7a and b that all the characteristic peaks move to lower degrees after reaction, indicating the d-spacings is increased. The change of d-spacing accompanying with the incorporation of Cu<sup>2+</sup> or Cr<sup>3+</sup> can be caused by the anion exchanges in the interlayers or the isomorphous substitution in the plate [49,50]. Isomorphous substitution affects the layered framework because of the difference in ionic radius (66 pm for Mg<sup>2+</sup>, 72 pm for Cu<sup>2+</sup>, 64 pm for Cr<sup>3+</sup> and 55 pm for Al<sup>3+</sup>). The structure of Cu<sup>2+</sup> or Cr<sup>3+</sup> doped LDHs will be discussed in detail with the help of TEM and NMR analysis.

The ratio of dissolved metal ions to the immobilized ions (D/I ratio) in the solid-solution exchange reaction with LDHs is calculated as follow:

$$D/I \text{ ratio} = \frac{C_{\text{dissolved}}}{C_{\text{immobilized}}} \tag{6}$$

It can be concluded that the D/I ratio of Cr<sup>3+</sup> ion reaches 0.962, indicating a uniform substitution. It seems that Cr ions are homogeneously distributed at previous Al sites in the main plate. The D/I ratio of Cu<sup>2+</sup> ion is 0.246 indicating that the amount of immobilized Cu<sup>2+</sup> ion is more than the dissolved Mg<sup>2+</sup> ion. The chemical composition of Cu<sup>2+</sup> or Cr<sup>3+</sup> doped LDHs can be determined from Table 3.

Based on the assumption that a homogeneous phase is generated, and the possible chemical formula of products after immobilization can be calculated from the ICP results and initial molar fraction of C-LDHs. 2 g of C-LDHs (6.875 mmol) contain 27.5 mmol Mg ions and 13.75 mmol Al ions in the main plates according to its structural formula. After exchange with Cr<sup>3+</sup> ions, 1.458 mmol Al<sup>3+</sup> ions are dissolved into the solution and 1.5 mmol Cr ions are immobilized into the main plate. There are thus 27.5 mmol Mg ions, 12.25 mmol Al ions and 1.5 mmol Cr ions in the re-constructed main plate. Therefore, the possible chemical

Table 3  
Amount of metal ions dissolved and immobilized by LDHs.

Reaction	Immobilized (mM)		Dissolved (mM)		D/I ratio	Calculated chemical formula
	Cu <sup>2+</sup>	Cr <sup>3+</sup>	Mg <sup>2+</sup>	Al <sup>3+</sup>		
C-LDHs and Cu <sup>2+</sup>	4.533	–	1.117	–	0.246	Mg <sub>3.91</sub> Cu <sub>0.33</sub> Al <sub>2</sub> (OH) <sub>12</sub> CO <sub>3</sub> ·3H <sub>2</sub> O
C-LDHs and Cr <sup>3+</sup>	–	3.030	–	2.916	0.962	Mg <sub>4</sub> Al <sub>1.78</sub> Cr <sub>0.22</sub> (OH) <sub>12</sub> CO <sub>3</sub> ·3H <sub>2</sub> O

formula of  $\text{Mg}_4\text{Al}_{1.78}\text{Cr}_{0.22}(\text{OH})_{12}\text{CO}_3 \cdot 3\text{H}_2\text{O}$  can be obtained for the products containing  $\text{Cr}^{3+}$ . A possible chemical formula of  $\text{Mg}_{3.91}\text{Cu}_{0.33}\text{Al}_2(\text{OH})_{12}\text{CO}_3 \cdot 3\text{H}_2\text{O}$  is calculated for the products after the immobilization tests for  $\text{Cu}^{2+}$  ions following the same calculation procedure. The  $\text{M}^{2+}/\text{M}^{3+}$  molar ratio of rehydrated LDHs after the immobilization tests for  $\text{Cu}^{2+}$  ions is 2.12, which is slightly changed. The results suggest that  $\text{Cu}^{2+}$  ions in the solution are immobilized through both isomorphous substitution and formation of  $\text{Cu}^{2+}$  doped layer framework with a non-stoichiometric structure [15].

In order to further identify whether  $\text{Cr}^{3+}$  substitutes  $\text{Al}^{3+}$  in LDHs layered framework and whether homogeneous  $\text{Cu}^{2+}$  or  $\text{Cr}^{3+}$  doped LDHs is generated, the structure of layered framework after reacting with  $\text{Cr}^{3+}$  ions is analyzed with TEM. High resolution lattice image and electron diffraction pattern of LDHs reacting with  $\text{Cr}^{3+}$  ions are shown in Fig. 8. The software Digital Micrograph is used to calibrate the electron diffraction pattern, to measure the radius of each diffraction ring and to calculate corresponding d-spacing value. The calculated d-spacing values are compared

with pdf cards shown in Table 4 and the corresponding crystal indices are identified.

The TEM images of the LDHs show a plate-like morphology with no defined orientation. It can be seen from Table 4 that there exists a match between d value calculated from calibration of electron diffraction pattern and d-spacing in pdf card from standard material ( $\text{Mg}_6\text{Cr}_2\text{CO}_3(\text{OH})_{16} \cdot 4\text{H}_2\text{O}$ , PDF: 0045-1475). Therefore, new LDHs structure with a chemical formula of  $\text{Mg}_6\text{Cr}_2\text{CO}_3(\text{OH})_{16} \cdot 4\text{H}_2\text{O}$  can be identified from TEM analysis, which is not consistent with the results from D/I ratio tests by ICP, indicating the exchanged layered framework is heterogeneous in regard to the distribution of  $\text{Cr}^{3+}$  ions.

XPS is used to further characterize the isomorphous substitution of  $\text{Cu}^{2+}$  or  $\text{Cr}^{3+}$  ions into the structure of LDHs, as shown in Fig. 9. The high resolution XPS spectrum of  $\text{Cu}^{2+}$  2p shows the presence of four peaks at 935.2, 943.5, 954.3, and 963.0 eV. The binding energies of the  $\text{Cu}$   $2p_{3/2}$  and  $\text{Cu}$   $2p_{1/2}$  peak are 963.0 and 935.2 eV, whereas their shake-up satellite peaks are 954.3 and

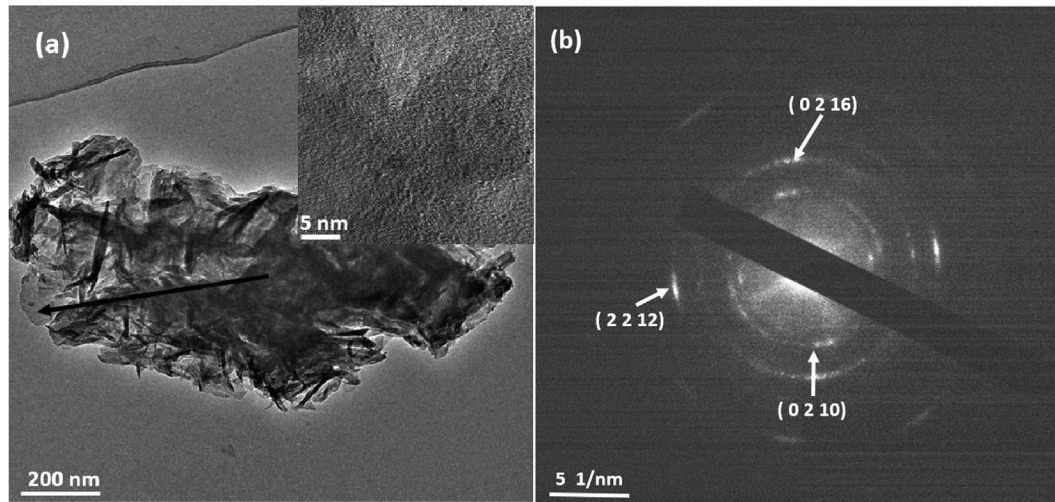


Fig. 8. TEM image and Electron diffraction pattern of LDHs containing  $\text{Cr}^{3+}$ . (a) High resolution lattice image, (b) Electron diffraction pattern.

Table 4  
Calculated d values and crystal indices.

Number	Radius of diffraction ring (nm)	d-spacing (nm)	d (hkl)	Plane (hkl)
1	7.0196	0.1425	0.1437	(2 2 12)
2	4.9406	0.2024	0.1976	(0 2 16)
3	4.1205	0.2427	0.2323	(0 2 10)

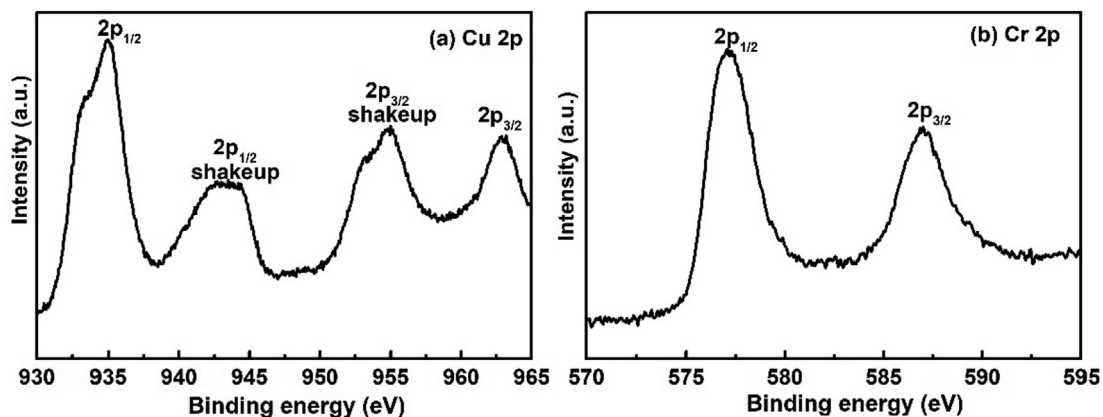


Fig. 9. XPS spectra of rehydrated C-LDHs after reaction with  $\text{Cu}^{2+}$  or  $\text{Cr}^{3+}$  solution. (a)  $\text{Cu}$  2p high resolution XPS spectra; (b)  $\text{Cr}$  2p high resolution XPS spectra.

943.5 eV, respectively [32]. The peaks of  $\text{Cr}^{3+}$  2p at 577.3 and 587.3 are observed from the high resolution XPS spectrum (Fig. 9b). The results from the XPS spectra of rehydrated LDHs suggest the isomorphous substitution of  $\text{Cu}^{2+}$  or  $\text{Cr}^{3+}$  ions into the LDHs structure.

Summarizing from the results and discussions above,  $\text{Cu}^{2+}$  or  $\text{Cr}^{3+}$  ions are immobilized in the form of isomorphous substitution and the  $\text{Cu}^{2+}$  or  $\text{Cr}^{3+}$  doped LDHs has a non-stoichiometric structure. The method of NMR analysis combined with first principle calculations are employed to reveal the inter-atomic interactions and the consequent atomic arrangements in the non-stoichiometric structure.

$^{27}\text{Al}$  and  $^1\text{H}$  NMR spectra for LDHs samples reacting with  $\text{Cu}^{2+}$  or  $\text{Cr}^{3+}$  ions are shown in Fig. 10. The peaks at 8–10 ppm in  $^{27}\text{Al}$  NMR spectra correspond to octahedral  $\text{Al}(\text{OH})_6$  structural unit in the plate and slightly move to higher chemical shift after reaction with  $\text{Cu}^{2+}$  or  $\text{Cr}^{3+}$  ions, which indicates small alteration of chemical environments of Al atoms. Since NMR signals are determined by nearest-neighbor atoms while slightly affected by second-nearest-neighbor atoms,  $^{27}\text{Al}$  NMR spectra are not effective to clarify alteration of LDHs structure induced by reaction with  $\text{Cu}^{2+}$ ,  $\text{Cr}^{3+}$  ions.

$^1\text{H}$  NMR spectra are sensitive to reflect slight changes of LDHs structure [25]. Two chemical environments of H atoms of O-LDHs are observed in  $^1\text{H}$  NMR spectra at 3.6 and 0.2 ppm, which are attributed to  $\text{Mg}_3\text{-OH}$  and  $\text{Mg}_2\text{Al-OH}$  [15], respectively. The peaks at 5.3 ppm correspond to  $\text{H}_2\text{O}$  molecule in the structure of LDHs [25]. More peaks around 2.8 and 2.3 ppm are detected in  $^1\text{H}$

NMR spectra for LDHs reacted with Cu and Cr ions. The peaks around 2.8 and 2.3 ppm are interpreted with the help of first principle calculations rooting in DFT-GIPAW methods.

### 3.3. First principle calculations for NMR results

The unit cell of O-LDHs is built based on the unit of Brucite [51], which is shown in Fig. 11. The unit cell of Brucite is prolonged along the c axis to 0.772 nm firstly. Afterwards, the Mg atoms at vertex is substituted by Al atoms and chlorides anions are put into the interlayer of  $\text{Mg}(\text{OH})_2$  layers. The final unit cell of O-LDHs is obtained after geometry optimization performed with CASTEP (also using a k point grip of  $3 \times 3 \times 1$  and cut off energy of 500 eV) [52,53]. The parameters of unit cell after geometry optimization is listed in Table 5. The periodical models of  $\text{Cu}^{2+}$  or  $\text{Cr}^{3+}$  doped LDHs are built based on O-LDHs with the above three steps. Water molecules are ignored for increasing the calculation efficiency.

**Table 5**  
Calculated geometrical parameters and experimental values for O-LDHs.

	Calculated	Experiment (Dong, Zhang et al. 2015)
a (Å)	6.286	6.130
c (Å)	7.770	7.720
Mg-O (Å)	2.121	2.100
Al-O (Å)	1.956	2.000
O-H (Å)	0.995	1.000

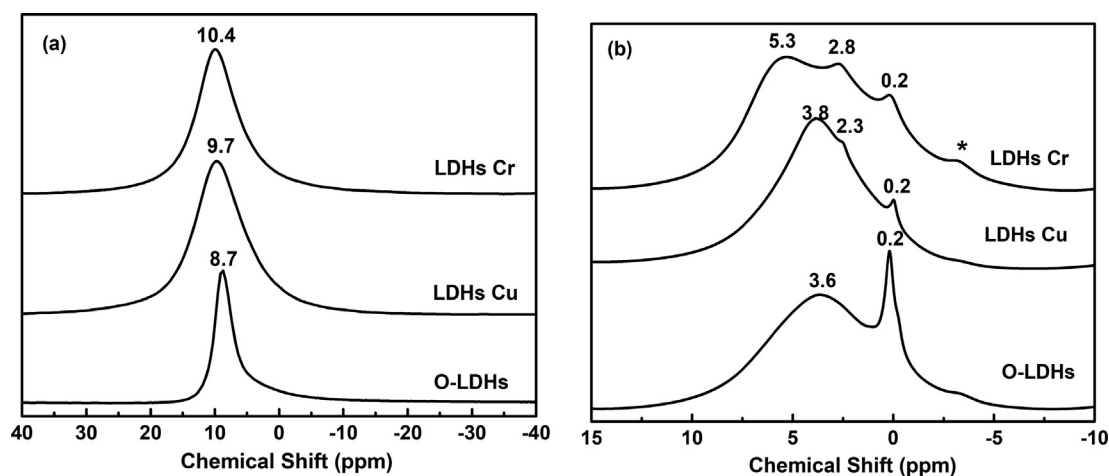


**Fig. 10.**  $^{27}\text{Al}$  and  $^1\text{H}$  NMR spectra for LDHs containing  $\text{Cu}^{2+}$  or  $\text{Cr}^{3+}$  ions. (a)  $^{27}\text{Al}$  NMR spectra, (b)  $^1\text{H}$  NMR spectra \* indicates spinning sidebands.

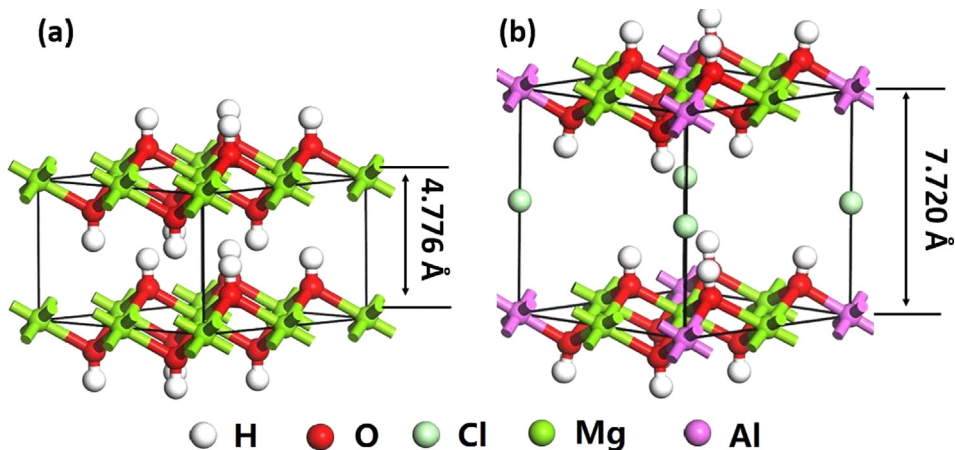


**Fig. 11.** Unit cell of Brucite and O-LDHs. (a) Brucite, (b) LDHs.

At the molecular level, LDHs consists of single layers formed by a hexagonal “honeycomb” arrangement of metal cations with hydroxyl groups pointing alternatively up and down perpendicular to the plane of the sheet. Mg atoms build a hexagonal two-

dimensional (2D) pattern while Al-OH-Al linkages are absent in the hydroxide layers. Therefore, there are four possible environments of H atoms in  $\text{Cu}^{2+}$  doped LDHs, which are  $\text{Mg}_3\text{-OH}$ ,  $\text{Mg}_2\text{-Cu-OH}$ ,  $\text{MgCuAl-OH}$  and  $\text{Mg}_2\text{Al-OH}$ . Another three environments

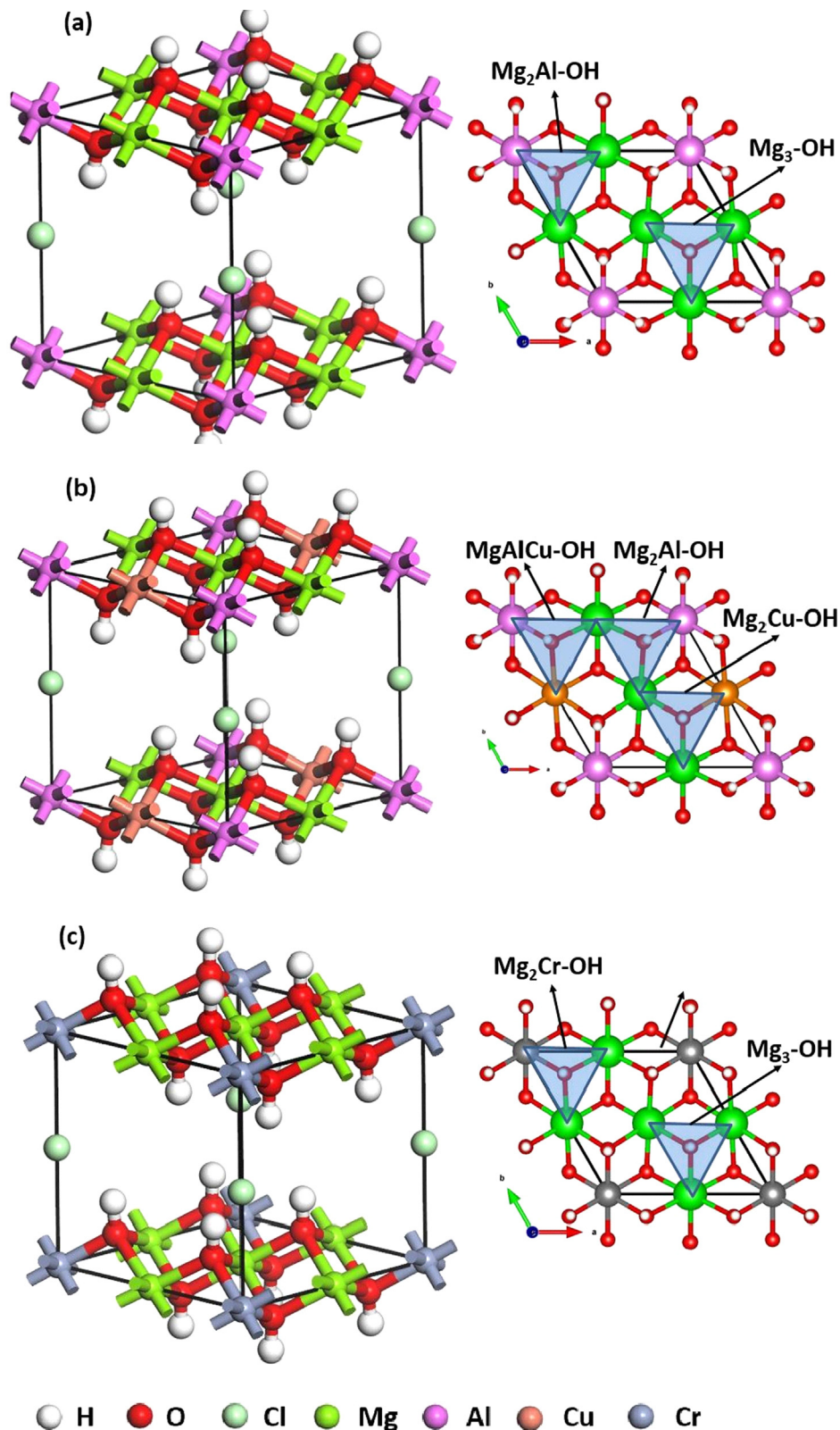
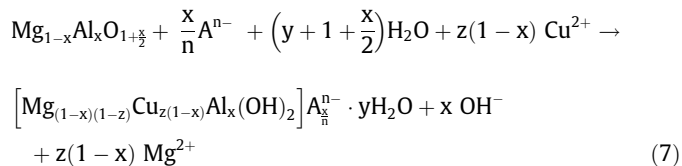


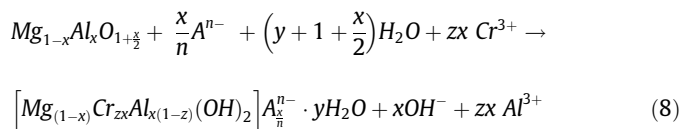
Fig. 12. Unit cell and chemical environments of H atoms of LDHs. (a) O-LDHs, (b) LDHs Cu, (c) LDHs Cr.

of H atoms are supposed to be observed in Cr<sup>3+</sup> doped LDHs, which are Mg<sub>3</sub>-OH, Mg<sub>2</sub>Cr-OH, Mg<sub>2</sub>Al-OH. All of these environments of H atoms are present in the unit cell of Cu-LDHs and Cr-LDHs built with Material Studio (Fig. 12). First principle calculations of NMR chemical shifts are performed to interpret the NMR signals, and the results of calculation are listed in Table 6. The calculated chemical shifts based on <sup>1</sup>H NMR analysis (Table 6) are close to the values obtained in the experiments (Fig. 10), indicating a high precision of the DFT based calculation [54]. The chemical shifts of H atoms with environments of Mg<sub>2</sub>Cu-OH and MgCuAl-OH are 0.10 and 2.79, respectively. Combining the calculation and the NMR experiment (Table 6), the peak around 2.3 ppm in LDHs reacting with Cu<sup>2+</sup> ions is assigned to H atoms with chemical environment of MgCuAl-OH, while the peak around 0.2 ppm can be assigned to Mg<sub>2</sub>Cu-OH and Mg<sub>3</sub>-OH. The peak around 2.8 ppm in Cr<sup>3+</sup> doped LDHs is assigned to H atoms with chemical environment of Mg<sub>2</sub>Cr-OH. The results of NMR tests and first principle calculations also suggest the immobilization mechanism of isomorphous substitution and formation of doped layer framework.

The Cu<sup>2+</sup> cations are immobilized through the mechanism of isomorphous substitution during the structure reconstruction of C-LDHs, while the Cu<sup>2+</sup> cations are only immobilized by surface adsorption and precipitation with O-LDHs [19]. The results suggest that heavy metal ions are more likely immobilized in the main plate of LDHs through isomorphous substitution during the structural reconstruction. Moreover, the structure of Cu<sup>2+</sup> doped LDHs can be represented as [Mg<sub>(1-x)</sub>Cr<sub>z</sub>Al<sub>x(1-z)</sub>Cu<sub>z(1-x)</sub>Al<sub>x</sub>(OH)<sub>2</sub>] A<sub>x/n</sub><sup>n-</sup> · yH<sub>2</sub>O, where z is the Cu<sup>2+</sup>/Mg<sup>2+</sup> molar ratio; and the immobilization of Cu can be expressed as below:



The structure of Cr<sup>3+</sup> doped LDHs can be represented as [Mg<sub>(1-x)Cr<sub>z</sub>Al<sub>x(1-z)</sub>(OH)<sub>2</sub>] A<sub>x/n</sub><sup>n-</sup> · yH<sub>2</sub>O, where z is the Cr<sup>3+</sup>/Al<sup>3+</sup> molar ratio, and the immobilization of Cu can be expressed as below:</sub>



### 3.4. Feasibility of using LDHs to immobilize heavy metal ions in cementitious materials

Compressive strength of the plain mortar and LDHs modified mortar cured for 14 days is shown in Fig. 13. It can be seen that adding C-LDHs slightly increases the compressive strength of mortar samples. The strength enhancement is due to the absorption of water during the rehydration of C-LDHs, leading to slightly reduced water to binder ratio.

Concentration of heavy metal ions in leached liquids from C-LDHs modified mortar is shown in Table 7. Quantities of leached heavy metal ions are reduced significantly in C-LDHs modified mortars. Heavy metal ions are reported to be immobilized by hydroxide precipitation in cementitious material matrix, because of the high alkaline pore solution [6,14]. Adding C-LDHs clearly enhance the immobilization of Cu<sup>2+</sup> and Cr<sup>3+</sup> in cementitious materials. These results bring hopes that by using slags rich in Mg, though they may contain remarkable amount of heavy metals, formation of LDHs from the Mg from slag and Al from Portland clinker

**Table 6**  
Calculated <sup>1</sup>H chemical shifts and experiment values.

Chemical environments	Calculated	Experiment
Mg <sub>3</sub> -OH	0.11	0.2
Mg <sub>2</sub> Cu-OH	0.10	0.2
MgCuAl-OH	2.79	2.3
Mg <sub>2</sub> Cr-OH	2.99	2.8
Mg <sub>2</sub> Al-OH	3.45	3.6

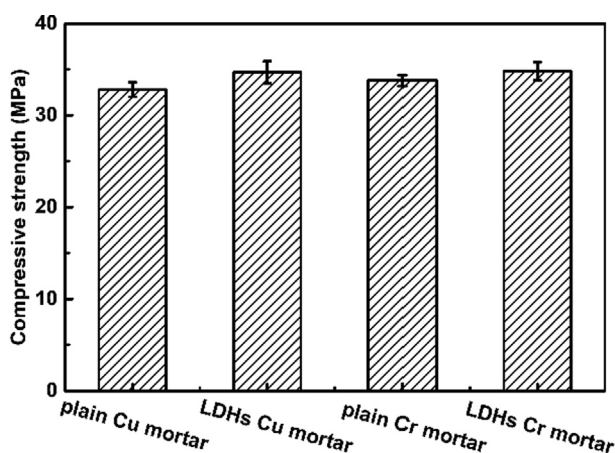


**Fig. 13.** Compressive strength of plain mortar and LDHs modified mortar at 14 days.

**Table 7**  
Concentration of metal ions in leachate from C-LDHs modified mortar (mM).

Ions	Plain mortar	LDHs modified mortar
Cu <sup>2+</sup>	0.661	0.299
Cr <sup>3+</sup>	1.904	1.192

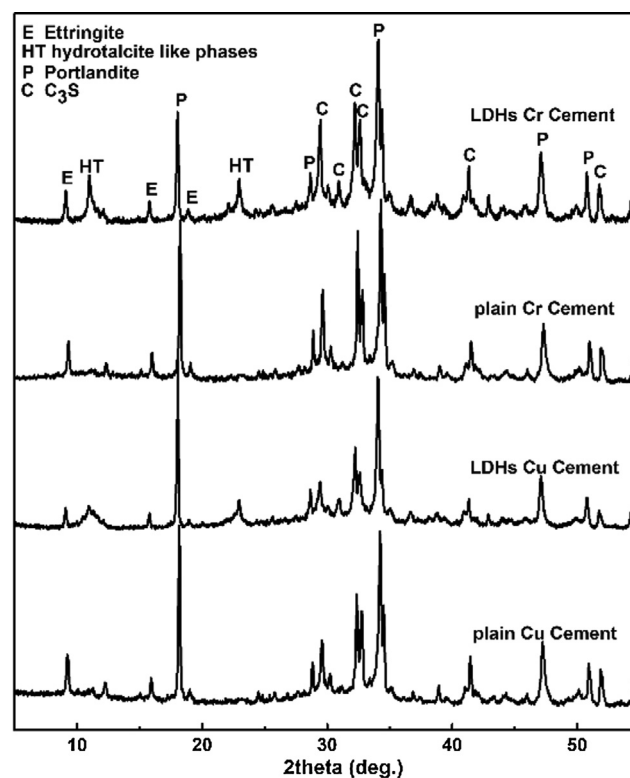


**Fig. 14.** XRD patterns of LDHs modified cement pastes containing Cu<sup>2+</sup> or Cr<sup>3+</sup> ions.

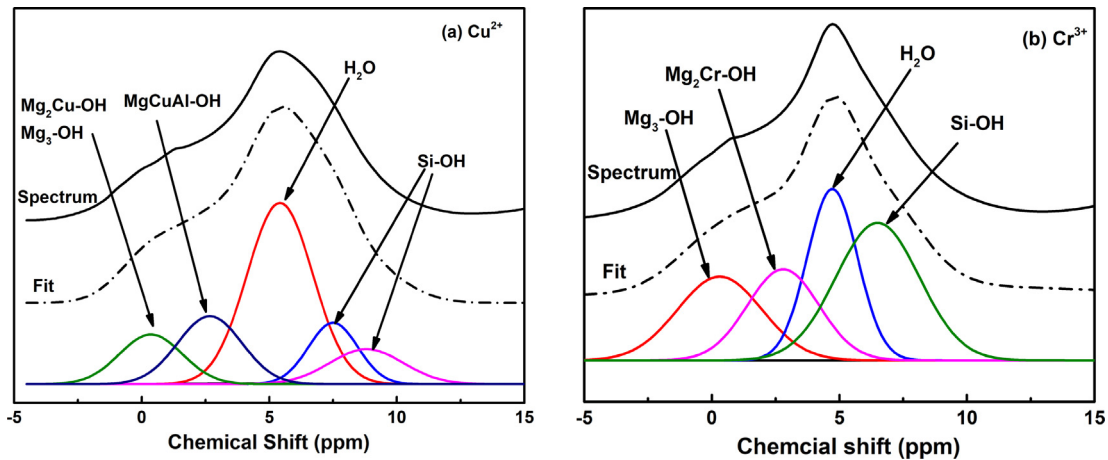


Fig. 15. Deconvolution of  $^1\text{H}$  NMR spectra of LDHs modified cement pastes containing  $\text{Cu}^{2+}$  or  $\text{Cr}^{3+}$  ions. (a)  $\text{Cu}^{2+}$ , (b)  $\text{Cr}^{3+}$ .

or slag can immobilize a significant amount of heavy metal ions. The risk of leaching heavy metals from the cementitious materials containing waste slag could thus be overestimated if the formation of LDHs and the consequent heavy metal binding capacities provided by the LDHs is ignored. Using slags rich in Mg can also be a possible solution for mitigating the risk of heavy metal leaching whenever admixtures containing heavy metals are used in cement production.

The immobilization mechanism and the location of  $\text{Cu}^{2+}$  or  $\text{Cr}^{3+}$  in C-LDHs modified cement are investigated with XRD and  $^1\text{H}$  NMR. Ettringite, Portlandite and residual  $\text{C}_3\text{S}$  are identified in plain cement pastes containing  $\text{Cu}^{2+}$  or  $\text{Cr}^{3+}$  ions (Fig. 14). Peaks of Ettringite, and Portlandite are observed in all patterns, which are typical hydration products of Portland cement. The characteristic peaks of hydrotalcite-like phases are also detected in the patterns of LDHs modified cement pastes, which are resulting from rehydration of C-LDHs in cement [40]. Some shifts of these characteristic peaks of hydrotalcite-like phases are observed due to isomorphous substitution and disordered sites during the formation of layered structure. No heavy metal hydroxides and metal carbonates are detected. It is most likely that hydrotalcite-like phases leads to the enhanced immobilization of  $\text{Cu}^{2+}$  and  $\text{Cr}^{3+}$  in cementitious materials.

$^1\text{H}$  NMR spectra of C-LDHs modified cement pastes containing  $\text{Cu}^{2+}$  or  $\text{Cr}^{3+}$  ions are shown in Fig. 15. The peak around 5 ppm are assigned to  $\text{H}_2\text{O}$  molecule in the structure of C-S-H gels, while the peaks around 7.1 and 8.5 ppm are assigned to Si-OH groups or Si-OH...Ca groups. Moreover, H atoms located at MgCuAl-OH,  $\text{Mg}_2\text{Cu-OH}$  and  $\text{Mg}_2\text{Cr-OH}$  are also identified in the pastes which further proves that  $\text{Cu}^{2+}$  or  $\text{Cr}^{3+}$  ions are immobilized as layered hydrotalcite-like structures.

#### 4. Conclusion

The uptake mechanism of heavy metal ions in calcinated LDHs during the rehydration process are studied in this paper. The inter-atomic interactions and the consequent atomic re-arrangements in the plate of LDHs after the rehydration process are revealed experimentally with NMR analysis based on outputs of first-principle calculations. The following conclusions can be drawn based on the outputs of experimental study and simulation work:

1.  $\text{Cu}^{2+}$  or  $\text{Cr}^{3+}$  ions in an aqueous solution can be efficiently immobilized with calcinated Mg-Al LDHs during its rehydration process. Calcinated LDHs show more effective immobilization effect than O-LDHs. The reaction kinetics of  $\text{Cu}^{2+}$  follows the

pseudo second-order type reaction and the saturated uptake capacity ( $q_e$ ) of  $\text{Cu}^{2+}$  in calcinated LDHs is about 11.3 mg/g.

2.  $\text{Cu}^{2+}$  or  $\text{Cr}^{3+}$  enters the plate of LDHs through isomorphous substitution for  $\text{Mg}^{2+}$  or  $\text{Al}^{3+}$  and forms a  $\text{Cu}^{2+}$  or  $\text{Cr}^{3+}$  doped layer framework with a non-stoichiometric structure.
3. The structure of  $\text{Cu}^{2+}$  doped LDHs is identified as  $[\text{Mg}_{(1-x)}\text{Cu}_{(1-x)z}\text{Al}_x^{3+}(\text{OH})_2]\text{A}_{x/n}^{n-}\cdot y\text{H}_2\text{O}$ , where  $z$  is the  $\text{Cu}^{2+}/\text{Mg}^{2+}$  molar ratio. The structure of  $\text{Cr}^{3+}$  doped LDHs is identified as  $[\text{Mg}_{1-x}^{2+}\text{Cr}_x^{3+}\text{Al}_x^{3+}(\text{OH})_2]\text{A}_{x/n}^{n-}\cdot y\text{H}_2\text{O}$ , where  $z$  is the  $\text{Cr}^{3+}/\text{Al}^{3+}$  molar ratio.
4.  $\text{Cu}^{2+}$  and  $\text{Cr}^{3+}$  ions are efficiently immobilized by the reconstruction process of calcinated LDHs in cement.  $\text{Cu}^{2+}$  or  $\text{Cr}^{3+}$  ions are immobilized with the formation of a substitutional solid solution in the layered structure of hydrotalcite-like phases.
5. Using slags rich in Magnesium could potentially be an effective solution for mitigating the risk of heavy metal leaching by forming LDHs in the hydration products in cementitious materials.

#### Declaration of Competing Interest

None.

#### Acknowledgments

This research has been financially supported by the National Natural Science Foundation of China (project 51672199), the Fundamental Research Funds for the Central Universities (WUT: 2017-YB-008), National Key Research and Development Program of China (Project 2016YFB0303501). The author thanks Dr. Xiaoyun Li from State Key Laboratory of Silicate Materials for Architectures and Chaofeng He, Yunyun Zou from Shiyanjia Laboratory ([www.shiyanjia.com](http://www.shiyanjia.com)) for the assistance with the NMR tests.

#### References

- [1] K.S. Wang, K.L. Lin, Z.Q. Huang, Hydraulic activity of municipal solid waste incinerator fly-ash-slag-blended eco-cement, *Cem. Concr. Res.* 31 (1) (2001) 97–103.
- [2] K.L. Lin, The influence of municipal solid waste incinerator fly ash slag blended in cement pastes, *Cem. Concr. Res.* 35 (5) (2005) 979–986.
- [3] H.S. Shi, L.L. Kan, Leaching behavior of heavy metals from municipal solid wastes incineration (MSWI) fly ash used in concrete, *J. Hazard. Mater.* 164 (2–3) (2009) 750–754.
- [4] X.Z. Zhu, X.N. Wu, J. Yao, F. Wang, W.J. Liu, Y.Y. Luo, et al., Toxic effects of binary toxicants of cresol frother and Cu (II) on soil microorganisms, *Int. Biodeterior. Biodegr.* 128 (2018) 155–163.
- [5] Q.Y. Chen, M. Tyrer, C.D. Hills, X.M. Yang, P. Carey, Immobilisation of heavy metal in cement-based solidification/stabilisation: a review, *Waste Manage.* 29 (1) (2009) 390–403.

- [6] J. Deja, Immobilization of  $\text{Cr}^{6+}$ ,  $\text{Cd}^{2+}$ ,  $\text{Zn}^{2+}$  and  $\text{Pb}^{2+}$  in alkali-activated slag binders, *Cem. Concr. Res.* 32 (12) (2002) 1971–1979.
- [7] S. Peysson, J. Pera, M. Chabannet, Immobilization of heavy metals by calcium sulfoaluminate cement, *Cem. Concr. Res.* 35 (12) (2005) 2261–2270.
- [8] B.I. Ei-Eswed, O.M. Aldagag, F.I. Khalili, Efficiency and mechanism of stabilization/solidification of  $\text{Pb}(\text{II})$ ,  $\text{Cd}(\text{II})$ ,  $\text{Cu}(\text{II})$ ,  $\text{Th}(\text{IV})$  and  $\text{U}(\text{VI})$  in metakaolin based geopolymers, *Appl. Clay Sci.* 140 (2017) 148–156.
- [9] C.K. Park, Hydration and solidification of hazardous wastes containing heavy metals using modified cementitious materials, *Cem. Concr. Res.* 30 (3) (2000) 429–435.
- [10] M.L. Ward, G. Bitton, T. Townsend, Heavy metal binding capacity (HMBC) of municipal solid waste landfill leachates, *Chemosphere* 60 (2) (2005) 206–215.
- [11] Z. Giergiczny, A. Krol, Immobilization of heavy metals ( $\text{Pb}$ ,  $\text{Cu}$ ,  $\text{Cr}$ ,  $\text{Zn}$ ,  $\text{Cd}$ ,  $\text{Mn}$ ) in the mineral additions containing concrete composites, *J. Hazard. Mater.* 160 (2–3) (2008) 247–255.
- [12] C.E. Halim, R. Amal, D. Beydoun, J.A. Scott, G. Low, Implications of the structure of cementitious wastes containing  $\text{Pb}(\text{II})$ ,  $\text{Cd}(\text{II})$ ,  $\text{As}(\text{V})$ , and  $\text{Cr}(\text{VI})$  on the leaching of metals, *Cem. Concr. Res.* 34 (7) (2004) 1093–1102.
- [13] J.Y. Chen, Y.H. Wang, H.Q. Wang, S. Zhou, H.D. Wu, X.R. Lei, Detoxification/immobilization of hexavalent chromium using metakaolin-based geopolymer coupled with ferrous chloride, *J. Environ. Chem. Eng.* 4 (2) (2016) 2084–2089.
- [14] C. Fan, B. Wang, T. Zhang, Review on cement stabilization/solidification of municipal solid waste incineration fly ash, *Adv. Mater. Sci. Eng.* 2018 (2018).
- [15] S. Cadars, G. Layrac, C. Gerardin, M. Deschamps, J.R. Yates, D. Tichit, et al., Identification and quantification of defects in the cation ordering in Mg/Al layered double hydroxides, *Chem. Mater.* 23 (11) (2011) 2821–2831.
- [16] Y.S. Zhang, W. Sun, Q.L. Chen, L. Chen, Synthesis and heavy metal immobilization behaviors of slag based geopolymer, *J. Hazard. Mater.* 143 (1–2) (2007) 206–213.
- [17] Q.H. Guo, J. Tian, Removal of fluoride and arsenate from aqueous solution by hydrocalumite via precipitation and anion exchange, *Chem. Eng. J.* 231 (2013) 121–131.
- [18] M.C. Richardson, P.S. Braterman, Cation exchange by anion-exchanging clays: the effects of particle aging, *J. Mater. Chem.* 19 (42) (2009) 7965–7975.
- [19] M. Park, C.L. Choi, Y.J. Seo, S.K. Yeo, J. Choi, S. Komarneni, et al., Reactions of  $\text{Cu}^{2+}$  and  $\text{Pb}^{2+}$  with Mg/Al layered double hydroxide, *Appl. Clay Sci.* 37 (1–2) (2007) 143–148.
- [20] T. Kameda, H. Takeuchi, T. Yoshioka, Uptake of heavy metal ions from aqueous solution using Mg-Al layered double hydroxides intercalated with citrate, malate, and tartrate, *Sep. Purif. Technol.* 62 (2) (2008) 330–336.
- [21] T. Kameda, S. Saito, Y. Umetsu, Mg-Al layered double hydroxide intercalated with ethylene-diaminetetraacetate anion: Synthesis and application to the uptake of heavy metal ions from an aqueous solution, *Sep. Purif. Technol.* 47 (1–2) (2005) 20–26.
- [22] X.F. Liang, Y.B. Zang, Y.M. Xu, X. Tan, W.G. Hou, L. Wang, et al., Sorption of metal cations on layered double hydroxides, *Colloid Surface A.* 433 (2013) 122–131.
- [23] S. Komarneni, N. Kozai, R. Roy, Novel function for anionic clays: selective transition metal cation uptake by diadochy, *J. Mater. Chem.* 8 (6) (1998) 1329–1331.
- [24] Y.X. Chen, Z.H. Shui, W. Chen, G.W. Chen, Chloride binding of synthetic Ca-Al-NO<sub>3</sub> LDHs in hardened cement paste, *Constr. Build. Mater.* 93 (2015) 1051–1058.
- [25] P.J. Sideris, U.G. Nielsen, Z.H. Gan, C.P. Grey, Mg/Al ordering in layered double hydroxides revealed by multinuclear NMR spectroscopy, *Science* 321 (5885) (2008) 113–117.
- [26] M. Profeta, F. Mauri, C.J. Pickard, Accurate first principles prediction of O-17 NMR parameters in  $\text{SiO}_2$ : assignment of the zeolite ferrierite spectrum, *J. Am. Chem. Soc.* 125 (2) (2003) 541–548.
- [27] M. Profeta, M. Benoit, F. Mauri, C.J. Pickard, First-principles calculation of the O-17 NMR parameters in Ca oxide and Ca aluminosilicates: the partially covalent nature of the Ca-O bond, a challenge for density functional theory, *J. Am. Chem. Soc.* 126 (39) (2004) 12628–12635.
- [28] S.E. Ashbrook, A.J. Berry, D.J. Frost, A. Gregorovic, C.J. Pickard, J.E. Readman, et al., O-17 and Si-29 NMR parameters of  $\text{MgSiO}_3$  phases from high-resolution solid-state NMR spectroscopy and first-principles calculations, *J. Am. Chem. Soc.* 129 (43) (2007) 13213–13224.
- [29] E. Lee, K.A. Persson, Li Absorption and Intercalation in Single Layer Graphene and Few Layer Graphene by First Principles, *Nano Lett.* 12 (4624) (2012) 8.
- [30] E. Kioupakis, P. Rinke, A. Schleife, F. Bechstedt, C.G.V.D. Walle, Free-carrier absorption in nitrides from first principles, *Phys. Rev. B.* 81 (2010) 2412011–2412014.
- [31] P. Duan, Research on Modification Mechanism and Application of Layered Double Hydroxides for Durability of Concrete, Wuhan University of Technology, Wuhan, 2014.
- [32] Y. Xiao, M. Sun, L. Zhang, X. Gao, J. Su, H. Zhu, The co-adsorption of  $\text{Cu}^{2+}$  and  $\text{Zn}^{2+}$  with adsorption sites surface-lattice reforming on calcined layered double hydroxides, *RSC Adv.* 5 (2015) 28369–28378.
- [33] N.K. Lazaridis, D.D. Asouhidou, Kinetics of sorptive removal of chromium(VI) from aqueous solutions by calcined Mg-Al hydrotalcite, *Water Res.* 37 (2003) 2875–2882.
- [34] S.A. Bernal, J.L. Provis, Durability of alkali-activated materials: progress and perspectives, *J. Am. Ceram. Soc.* 97 (4) (2014) 997–1008.
- [35] W. Chen, B. Li, Q. Li, J. Tian, Effect of polyaluminum chloride on the properties and hydration of slag-cement paste, *Constr. Build. Mater.* 124 (2016) 1019–1027.
- [36] J.E. Aubert, B. Husson, A. Vaquier, Use of municipal solid waste incineration fly ash in concrete, *Cem. Concr. Res.* 34 (6) (2004) 957–963.
- [37] M. Cyr, M. Coutand, P. Clastes, Technological and environmental behavior of sewage sludge ash (SSA) in cement-based materials, *Cem. Concr. Res.* 37 (8) (2007) 1278–1289.
- [38] L. Bertolini, M. Carsana, D. Cassago, A. Quadrio Curzio, M. Collepardi, MSWI ashes as mineral additions in concrete, *Cem. Concr. Res.* 34 (10) (2004) 1899–1906.
- [39] M.J. dos Reis, F. Silverio, J. Tronto, J.B. Valim, Effects of pH, temperature, and ionic strength on adsorption of sodium dodecylbenzenesulfonate into Mg-Al- $\text{CO}_3$  layered double hydroxides, *J. Phys. Chem. Solids* 65 (2–3) (2004) 487–492.
- [40] X.Y. Ke, S.A. Bernal, J.L. Provis, Controlling the reaction kinetics of sodium carbonate-activated slag cements using calcined layered double hydroxides, *Cem. Concr. Res.* 81 (2016) 24–37.
- [41] X.Y. Ke, S.A. Bernal, J.L. Provis, Uptake of chloride and carbonate by Mg-Al and Ca-Al layered double hydroxides in simulated pore solutions of alkali-activated slag cement, *Cem. Concr. Res.* 100 (2017) 1–13.
- [42] M.A. Gonzalez, I. Pavlovic, C. Barriga,  $\text{Cu}(\text{II})$ ,  $\text{Pb}(\text{II})$  and  $\text{Cd}(\text{II})$  sorption on different layered double hydroxides. A kinetic and thermodynamic study and competing factors, *Chem. Eng. J.* 269 (2015) 221–228.
- [43] J. Zhang, Y. Xu, W. Li, J. Zhou, J. Zhao, G. Qian, et al., Enhanced remediation of Cr(VI)-contaminated soil by incorporating a calcined-hydrotalcite-based permeable reactive barrier with electrokinetics, *J. Hazard. Mater.* 239–240 (2012) 128–134.
- [44] M.S. Rahman, M.R. Islam, Effects of pH on isotherms modeling for  $\text{Cu}(\text{II})$  ions adsorption using maple wood sawdust, *Chem Eng J.* 149 (2009) 273–280.
- [45] D. Rai, L.E. Eary, J.M. Zachara, Environmental Chemistry of Chromium, *Sci. Total Environ.* 86 (1989) 15–23.
- [46] T. Charpentier, The PAW/GIPAW approach for computing NMR parameters: A new dimension added to NMR study of solids, *Solid State Nucl. Mag.* 40 (1) (2011) 1–20.
- [47] S. Ispas, T. Charpentier, F. Mauri, D.R. Neuville, Structural properties of lithium and sodium tetrasilicate glasses: Molecular dynamics simulations versus NMR experimental and first-principles data, *Solid State Sci.* 12 (2) (2010) 183–192.
- [48] M.A. Gonzalez, I. Pavlovic, R. Rojas-Delgado, C. Barriga, Removal of  $\text{Cu}^{2+}$ ,  $\text{Pb}^{2+}$  and  $\text{Cd}^{2+}$  by layered double hydroxide-humate hybrid. Sorbate and sorbent comparative studies, *Chem. Eng. J.* 254 (2014) 605–611.
- [49] I. Pavlovic, M.R. Perez, C. Barriga, M.A. Ulibarri, Adsorption of  $\text{Cu}^{2+}$ ,  $\text{Cd}^{2+}$  and  $\text{Pb}^{2+}$  ions by layered double hydroxides intercalated with the chelating agents diethylenetriaminepentaacetate and meso-2,3-dimercaptosuccinate, *Appl. Clay Sci.* 43 (1) (2009) 125–129.
- [50] Y.X. Chen, Z.H. Shui, W. Chen, Q. Li, G.W. Chen, Effect of MgO content, of synthetic slag on the formation of Mg-Al LDHs and sulfate resistance of slag-fly ash-clinker binder, *Constr. Build. Mater.* 125 (2016) 766–774.
- [51] A. Trave, A. Selloni, A. Goursot, D. Tichit, J. Weber, First principles study of the structure and chemistry of Mg-based hydrotalcite-like anionic clays, *J. Phys. Chem. B* 106 (47) (2002) 12291–12296.
- [52] S.E. Ashbrook, L. Le Polles, C.J. Pickard, A.J. Berry, S. Wimperis, I. Farnan, First-principles calculations of solid-state O-17 and Si-29 NMR spectra of  $\text{Mg}_2\text{SiO}_4$  polymorphs, *PCCP* 9 (13) (2007) 1587–1598.
- [53] Q. Xu, Z.M. Ni, J.H. Mao, First principles study of microscopic structures and layer-anion interactions in layered double hydroxides intercalated various univalent anions, *J. Mol. Struct.-Theochem.* 915 (1–3) (2009) 122–131.
- [54] F. Tielens, C. Gervais, J.F. Lambert, F. Mauri, D. Costa, Ab initio study of the hydroxylated surface of amorphous silica: a representative model, *Chem. Mater.* 20 (10) (2008) 3336–3344.